Conformers of Saturated Chains: Matrix Isolation, Structure, IR and UV Spectra of *n*-Si_4Me_{10}

Bo Albinsson, Hiroyuki Teramae, John W. Downing, and Josef Michl*

Dedicated to Professor H.-D. Scharf on the occasion of his 65th birthday

Abstract: Infrared and ultraviolet spectra of the *gauche* and *anti* conformers of matrix-isolated permethyl-*n*-tetrasilane have been obtained separately by taking advantage of thermally induced *gauche*-to-*anti* conversion and of wavelength-selective photochemical destruction of either conformer. The resolved UV spectrum of the *gauche* conformer provides the first piece of experimental evidence in favor of the recently proposed reinterpretation of conformational effects on tetrasilane electronic states. According to this, it is not the energy but the intensity of the lowest singlet excitation that changes dramatically as the SiSiSiSi dihedral angle is varied, as a result of an avoided crossing between $\sigma\sigma^*$ and $\sigma\pi^*$ states. Implications for the general understanding of sigma conjugation in simple terms are discussed. Unconstrained MP2/6-31G* optimization predicts the existence of a third backbone conformer (*ortho*), with a dihedral angle of about 90°. Its predicted (HF/3-21G*) mid-IR spectrum is indistinguishable from that of the *gauche* conformer, and the matrix-isolation spectra thus provide no evidence for or against its presence.

Keywords
ab initio calculations · conformation · sigma conjugation · matrix isolation · oligosilanes

Introduction

The conformations of the silicon-backbone polymers, peralkylated polysilanes[1] $(SiRR')_n$, have been of considerable interest both for fundamental reasons and because of the potential utility of these materials, and have been the subject of numerous studies.[1-3] Peralkylation endows polysilanes with stability and makes their use practical.

Conformational effects on the electronic spectra of these saturated polymers in the near-UV region are striking, particularly considering that the interconversion of conformers merely involves rotations around single bonds. In neat solids,[1,4] considerable shifts in the absorption bands have been noted as a function of backbone conformation, which depends both on the nature of the alkyl substituents and on temperature. In solution, photophysical behavior suggests that singlet excitation in polysilanes tends to localize on a relatively small number of silicon atoms in a way dictated by chain conformation.[1,5-7] It is therefore important to develop an understanding of the conformational properties and electronic spectra of the short chain analogues, peralkylated oligosilanes.

[*] Dr. B. Albinsson,[+] Dr. J. W. Downing, Prof. J. Michl
Department of Chemistry and Biochemistry
University of Colorado, Boulder, CO 80309-0215 (USA)
Fax: Int. code +(303)492-0799
e-mail: michl@eefus.colorado.edu
Dr. Hiroyuki Teramae
NTT Basic Research Laboratories
Morinosato, Atsugi, Kanagawa 243-01 (Japan)
e-mail: teramae@silicon.ntt.jp
[+] New address: Fysikalisk kemi, CTH
Chalmers Tekniska Högskola, 41296 Göteborg (Sweden)

Decamethyl-*n*-tetrasilane, $Me_3SiMe_2SiSiMe_2SiMe_3$, is the shortest peralkylated chain expected to show conformational isomerism in the backbone. It is natural to assume that the fundamental conformational properties of all saturated linear chains will be similar, and discussions of polysilane conformations have so far been couched in terms of the two forms usual in hydrocarbons, *gauche* and *anti* (often called *trans*), with both typically deviating somewhat from the ideal angles of ±60 and 180°, respectively. Prior to work in this laboratory, the only spectroscopic investigation[8] of the conformers of decamethyl-*n*-tetrasilane (*n*-Si_4Me_{10}) that we are aware of assumed the existence of a twisted *gauche* and a planar (C_{2h}) *anti* form. From the temperature dependence of solution IR and Raman spectra, it was concluded that the *anti* form is more stable by about 0.5 kcal mol^{-1}.

In a preliminary communication,[9] we reported that, according to Hartree–Fock ab initio theory with the 3-21G* basis set, the standard assumption is wrong in the case of Si_4Me_{10}, in that this chain has three pairs of enantiomeric conformers, with SiSiSiSi dihedral angles of about ±60 (*gauche*), ±90 (*ortho*), and ±165° (*anti*). We now report that this surprising result remains unchanged even in an unconstrained MP2/6-31G* optimization, which should provide a better description of nonbonded methyl–methyl interactions, as it permits some electron correlation. The result has received further support from ab initio calculations performed for another only moderately hindered four-atom chain, C_4F_{10}. These also predicted three conformers,[10] and their existence has recently been confirmed experimentally.[11] We are currently attempting to establish the scope of these unexpected results and to rationalize them in terms that are standard in molecular mechanics, that is, van der Waals and

 © VCH Verlagsgesellschaft mbH, D-69451 Weinheim, 1996 0947-6539/96/0205-0529 $ 15.00+.25/0

electrostatic interactions, superimposed on an intrinsic barrier to rotation.[12]

In a more general context, saturated silicon-based chains can be viewed as models for all saturated linear skeletons built from atoms of elements in Group 14 of the periodic table. Their structured and easily accessible electronic absorption and emission spectra make the conformational dependence of their electronic structure easier to investigate than that of hydrocarbons, yet, the underlying principles are presumably identical. The sensitivity of the oligosilane spectra to chain length, branching, and conformation calls attention to σ conjugation, that is, to the fact that σ bonds are not fully localized and thus have more in common with π bonds than often thought. It has been proposed[13] that bond delocalization is the root cause of the small intrinsic threefold barriers to rotation separating the conformers of saturated σ skeletons in the ground state even in the absence of steric encumbrance, and it clearly affects many of their other important properties, too.

Although the properties of small model systems can nowadays be calculated reliably by ab initio methods, these do not necessarily provide the degree of intuitive understanding that permits an immediate qualitative prediction for the next system of interest. Such understanding was largely provided for π systems by the Hückel,[14] PMO,[15] and Pariser–Parr–Pople[16] models. To some degree, it has been provided for σ systems by the extended Hückel model (cf. the concept of through-bond coupling[17]), by semiempirical models of the zero differential overlap type,[18] and by the natural bond analysis of ab initio wave functions.[19] However, particularly for long chains, most of these models are sufficiently complicated that they do not really provide the simple insight that is available for π systems from the Hückel model or the PMO model, which requires no computer at all. Perhaps it is impossible to account for the properties of the much more complicated σ systems in as lucid a manner, and efforts in this direction may be doomed.

Certainly the very simple Sandorfy C model,[20] immensely popular among physicists interested in polysilanes because it finds these σ orbital chains to be isoelectronic with the familiar π orbital chains of polyacetylene, is inadequate. Since it considers only the geminal and the vicinal resonance integrals between the sp^3 hybrid orbitals in the polymer backbone, which are invariant to rotation about bonds, it incorrectly predicts the electronic structure of polysilanes to be independent of their conformation.

We have been intrigued by σ conjugation and have already published some initial results for model oligosilanes,[9, 21–27] along three lines. First, we are measuring their spectroscopic and photophysical properties as a function of chain length and conformation; second, we are computing these properties by ab initio methods; and third, we are searching for simple models that would reproduce the results and would be helpful for high molecular weight polysilanes.[1]

Among the simple models, the ladder C model,[24, 26] a generalization of the Sandorfy C model that considers all resonance integrals between the backbone hybrid orbitals located at neighboring silicons in the polysilane chain, looked promising for a while. It reproduced the chain-length dependence of the energies of the intense $\sigma\sigma^*$ transitions of permethylated oligosilanes, and their conformational dependence.[26] Unfortunately, ab initio calculations showed subsequently that the agreement was

Presently, we provide full details of our experimental and computational results for the IR and UV spectra of Si_4Me_{10}. They confirm the suspicion[27] that the much more complicated ladder H model, which is not restricted to the backbone hybrid orbitals, is the simplest that could possibly describe the electronic structure of saturated skeletons correctly for all chain lengths and conformations.

Editorial Board Member:[*] *Josef Michl grew up in Prague, Czechoslovakia, and earned his degrees at Charles University and the Academy of Sciences with V. Horák, P. Zuman, and R. Zahradník. He did postdoctoral work with R. S. Becker, M. J. S. Dewar, A. C. Albrecht, J. Linderberg, and F. E. Harris. He emigrated from Czechoslovakia in 1968, taught at the University of Utah in 1970–1986, left for the University of Texas at Austin, and in 1991 moved to his present position at the University of Colorado, Boulder. He has been the editor of Chemical Reviews since 1984. His current research interests are modular chemistry (molecular-size construction kits), electronic structure and spectra, photochemistry, reactive intermediates, and gas-phase cluster ions.*

Argon, nitrogen (both from US Welding, 99.999% purity), or xenon (Spectra Gases, 99.99% purity) gas were used in the matrix isolation experiments. The matrix gas was deposited on a polished CsI or sapphire deposition window, depending on whether IR or UV spectra were to be recorded. Simultaneous IR and UV experiments were carried out by depositing the matrix mixture on a polished BaF_2 deposition window (UV cut-off at 150 nm and IR cut-off at 650 cm^{-1}). The deposition windows were mounted on the second stage of a closed-cycle helium refrigerator (Air Products Displex 202) in an oxygen-free copper sample holder which was maintained at temperatures between 12 and 30 K during deposition, depending on the particular experiment (vide infra). Si_4Me_{10} [28] held at temperatures between -20 and 0 °C was evaporated into the stream of inert gas at a flow rate of about 2 mmol h^{-1} producing matrices with matrix ratios estimated to be between 1:2000 (mid-IR and UV) and 1:100 (far IR). The matrix was irradiated at 12 K with either a low-pressure cadmium spectral lamp (Phillips 93107 E; 43710 cm^{-1}) or a home-built microwave-powered low-pressure iodine lamp (48500 cm^{-1}) with a Suprasil quartz window. A 1 inch air-saturated water filter was used with both lamps to reduce the heat load on the sample and to block unwanted 56090 cm^{-1} radiation from the iodine lamp.

Mid-IR and far-IR spectra were measured at 1 cm^{-1} resolution on Nicolet 800 and 20 F FTIR spectrometers, respectively. The mid-IR spectrometer was equipped with a wide-range nitrogen-cooled MCT detector and the far-IR vacuum spectrometer with a helium-cooled Ge bolometer (Infrared Laboratories). UV/Vis spectra were measured on a modified [29] Cary 17 spectrophotometer at a spectral bandwidth of 2 nm.

Quantum mechanical calculations were done on IBM RS 6000-550 and 590 workstations using the Turbomole [30] program and on a CRAY C90-16/512 supercomputer at the Pittsburgh Computing Center using the Gaussian 92 program [31]. The basis sets were 3-21 G* [32], 6-31 G* [33], and 6-311 G**(MC) [34], with Cartesian d functions. All MP2 calculations were done without freezing the core electrons. The geometry was optimized with and without the assumption of C_2 symmetry, with negligible differences in the results.

The potential energy as a function of the SiSiSiSi dihedral angle ω was calculated first with the HF/3-21 G* method by freezing ω at different values and optimizing all the other coordinates, starting with the optimized geometry at a previous value of ω. The initial choice of the other twelve dihedral angles was arbitrary. The potential energy curve was subsequently recomputed in the same fashion with the MP2/3-21 G* method, starting with the HF/3-21 G* geometries. Because of possible "chemical hysteresis" [35], this procedure does not guarantee that the lowest

© VCH Verlagsgesellschaft mbH, D-69451 Weinheim, 1996
0947-6539/96/0205-0530 $ 15.00+.25/0 Chem. Eur. J. 1996, 2, No. 5

energy path from one conformer to the next, and from a 180° dihedral angle to a 0° dihedral angle, will be found. However, unconstrained optimization was performed at both levels of calculation for the three significant local minima thus found. In the HF/3-21 G* results, all second derivatives were positive, and vibrational spectra of the conformers were calculated in the double harmonic approximation. We were unable to calculate the second derivatives at the MP2 level.

The backbone dihedral angles and energies of the conformers reported here are therefore correct at the levels of calculation used, but the lowest barriers between them may be even lower than those found presently. A very shallow fourth minimum initially appeared to be present at a dihedral angle of 0°, but it was soon found to have one negative second derivative in the HF/3-21 G* calculation. A purely downhill path was then found that joined this saddle point to the *gauche* minimum; this illustrates the pitfalls of the presently adopted procedure for searching for the lowest energy path. It was felt, however, that the use of more sophisticated procedures was not warranted for a molecule of this size. After all, the exact size of the very small computed barriers between the conformer minima has little credibility in view of the still rather approximate nature of the calculation.

The geometries of the three conformers were subsequently reoptimized with the MP2/6-31 G* method, and nearly identical results were obtained. Finally, their energies were calculated with the MP2/6-311 G** (MC) method using the MP2/6-31 G* geometries. The dihedral angles and energies are collected in Table 1.

It is quite probable that there are other low-energy conformers that differ by rotations of the methyl groups, and possibly even of the terminal trimethylsilyl groups. Since our primary interest is in the conformation of the silicon backbone, we made no attempt to investigate the existence of these additional conformers, and view the three conformer minima that have been identified as representatives of three families of conformers.

The CI calculation of the electronic excitation energy and oscillator strength as function of dihedral angle used the optimized ground-state geometries and included all single excitations from valence orbitals (CIS/3-21 G*).

Results

We have investigated the IR and UV spectra of matrix-isolated *n*-Si_4Me_{10} and resolved the contribution due to the *anti* conformer from those due to other conformers. All spectral assignments are based on ab initio calculations. The material is organized as follows:

1) Calculations suggest that three stable conformers separated by small barriers are to be expected.
2) Their computed IR spectra suggest that two of the three will be spectrally indistinguishable in the mid-IR region.
3) A matrix annealing study reveals evidence for the presence of two spectrally distinct sets of conformers, as anticipated from the calculations.
4) A search for the predicted distinctive but very weak far-IR peaks that would permit a further differentiation between the two expected twisted conformers fails and the separate existence of the two twisted conformers of Si_4Me_{10} remains experimentally unproven for the time being.
5) A matrix photochemistry study confirms the presence of two spectrally distinct conformers and permits a quantitative separation of their UV and IR spectra.
6) The resolved IR spectra are compared with those predicted; the more stable conformer is identified as *anti* (calculated dihedral angle, 162°), and the less stable conformer as a mixture of *gauche* (calculated dihedral angle, 53°) and *ortho* (calculated dihedral angle, 91°) forms, spectrally indistinguishable in the mid-IR and probably also the UV regions.
7) The resolved UV spectra provide the first piece of experimental evidence for the recently proposed reinterpretation[9, 27] of the effect of conformation on electronic excitation in Si_4Me_{10}.

1. The Calculated Potential Energy Curve: Figure 1 shows the relative potential energy (uncorrected for the negligible difference in zero-point energy) of Si_4Me_{10} as a function of the dihedral angle, ω. The geometry is optimized without constraints in the potential energy minima, and all coordinates except ω are optimized in the nonstationary points along the curve. The three curves were all obtained with the 3-21 G* basis set, with unconstrained HF optimization, MP2 (frozen core) single-point energies for the optimized HF geometries, and unconstrained MP2 optimization, respectively. Unconstrained optimization of the equilibrium geometries at the MP2/6-31 G* level did not change the results significantly. The optimized geometries are shown in Figure 2 and are similar to the HF/3-21 G* geometries communicated earlier.[9] The energies are collected in Table 1.

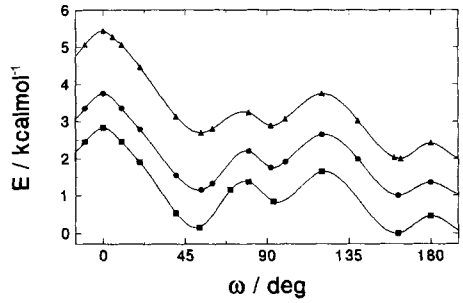

Fig. 1. Calculated ground-state potential energy of *n*-Si_4Me_{10} as a function of the SiSiSiSi dihedral angle, ω. From top to bottom: full HF/3-21 G* optimization, MP2 (frozen core) single-point energies for the HF optimized geometries, and full MP2/3-21 G* optimization. The three curves are offset by 1 kcal mol^{-1} at $\omega = 180°$ for clarity. The MP2/3-21 G* optimized values for the dihedral angle are 162.1 (*anti*), 93.4 (*ortho*), and 52.7° (*gauche*).

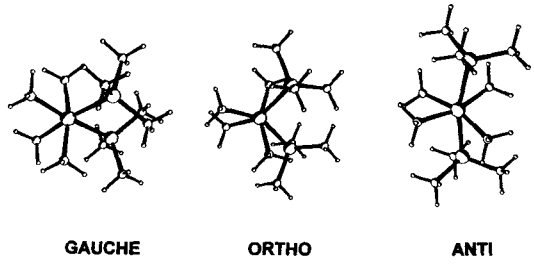

Fig. 2. Newman projections of the calculated geometries of the *gauche*, *ortho*, and *anti* conformers of Si_4Me_{10} (MP2/3-21 G*).

Table 1. Energies of the conformers of Si_4Me_{10}.

	anti	*ortho*	*gauche*
HF/3-21 G* [a]			
ω/°	163.5	92.0	53.7
E_{tot}/hartree	−1544.088312	−1544.086894	−1544.087204
E_{rel}/kcal mol^{-1}	0.00	0.89	0.70
MP2/3-21 G* [a]			
ω/°	162.1	93.1	52.7
E_{tot}/hartree	−1545.403971	−1545.402708	−1545.403788
E_{rel}/kcal mol^{-1}	0.00	0.79	0.11
MP2/6-31 G* [a]			
ω/°	161.7	91.4	52.6
E_{tot}/hartree	−1553.671902	−1553.670861	−1553.671761
E_{rel}/kcal mol^{-1}	0.00	0.65	0.09
MP2/6-311 G** [b]			
ω/°	161.7	91.4	52.6
E_{tot}/hartree	−1554.781281	−1554.780481	−1554.781004
E_{rel}/kcal mol^{-1}	0.00	0.50	0.17

[a] Fully optimized. [b] Single-point calculations at MP2/6-31 G* geometries.

The constancy of the results at all levels of theory suggests strongly that Si_4Me_{10} indeed has a total of at least six conformational minima whose energies lie within 1 kcal mol^{-1} of each other, and whose dihedral angles are near ± 162 (*anti*, *a*), ± 91 (*ortho*, *o*), and $\pm 53°$ (*gauche*, *g*). This can be contrasted with the situation in both *n*-butane and *n*-tetrasilane,[36] which have only three minima at 180 (*anti*, *a*) and about $\pm 60°$ (*gauche*, *g*). Elsewhere,[12] we attribute the origin of the splitting of the usual single twisted minimum into a pair of minima to 1,4-substituent interactions, as suggested for C_4F_{10}.[10]

2. Calculated IR Spectra: Since the best calculation (MP2/6-311G**//MP2/6-31G*) places the *gauche* conformer only 0.2 kcal mol^{-1} and the *ortho* conformer 0.5 kcal mol^{-1} above the *anti* conformer in energy, and predicts similar moments of inertia and vibrational frequencies, that is, small differences in entropy, all three conformers are expected to be detectable in gaseous Si_4Me_{10} at room temperature. As perfect annealing upon deposition on the cold window is unlikely,[37] they should all contribute to the observed matrix spectra.

Figure 3 shows the calculated (HF/3-21G*) and observed IR spectrum of Si_4Me_{10} deposited together with excess Xe on a 30 K CsI window. Most of the peaks are heavily overlapped, particularly in the methyl stretching (3000–2850 cm^{-1}) and deformation (1450–1200 cm^{-1}) regions, and also many of the silicon backbone modes. These provide no immediate information on individual conformers. However, in the 900–600 cm^{-1} region, where SiCH deformation and SiC stretching vibrations dominate, and in particular in the far-IR Si–Si stretching region (500–300 cm^{-1}), the three conformers have bands calculated to be separated by up to 5 cm^{-1} (Table 2). The *anti* species is easiest to distinguish in the spectra since its geometry is nearly inversion symmetric (at $\omega = 180°$, C_{2h}, all transitions to gerade states would be forbidden), and also because it differs the most in structure from the other two fairly compact forms. Unfortunately, in the far-IR Si–Si stretch region, where the spectra of all three conformers should be different enough to be observed directly, the calculated intensities are two orders of magnitude weaker than in the mid-IR region.

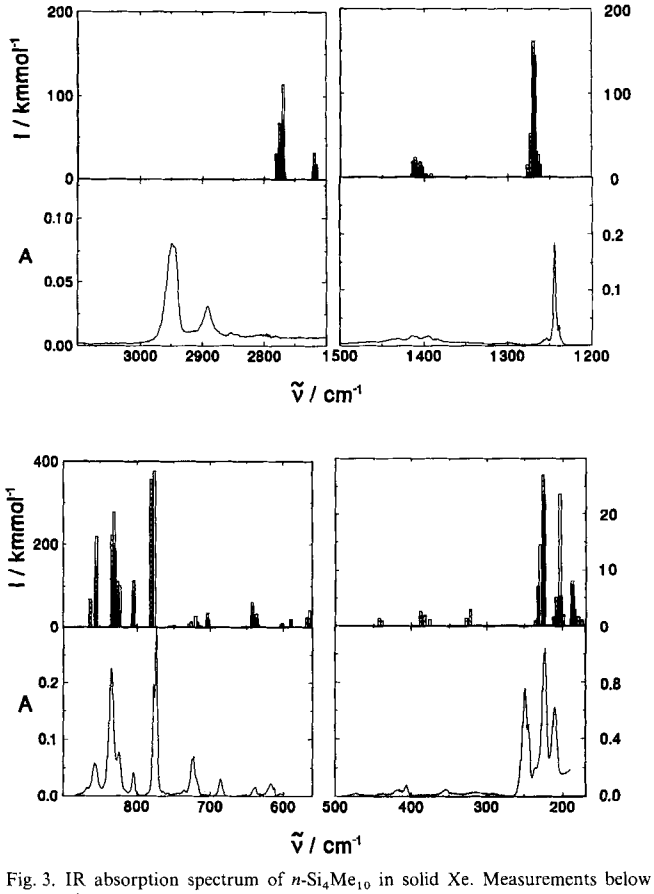

Fig. 3. IR absorption spectrum of *n*-Si_4Me_{10} in solid Xe. Measurements below 600 cm^{-1} were made on a matrix about 100 times more concentrated. The top panels show the IR spectrum calculated (HF/3-21G*, frequencies scaled by 0.86) for the *anti* (white sticks), *gauche* (hatched right up), and *ortho* (hatched left up) conformers of Si_4Me_{10}.

Table 2. Vibrations of *anti*, *ortho*, and *gauche* Si_4Me_{10}.

		Calcd [a]		Obsd [b]	
	no. [c]	$\tilde{\nu}$/cm^{-1}	I/km mol^{-1}	$\tilde{\nu}$/cm^{-1}	A [d]
asym. CH_3 str.	20	2766–2788	100 [e]	2949	26
sym. CH_3 str.	10	2715–2721	30 [e]	2892	10
asym. CH_3 def.	20	1395–1414	20 [e]	1435.8	4
				1431.7	4
				1413.7	5
				1394.4	5
				1386.1	3
				1383.2	3
sym. CH_3 def.	10	1260–1276	160 [e]	1244.5	59
				1238.8	12
SiCH def.	20	863.6 (*g*), 863.2 (*o*)	69, 46	867.4 (*o* + *g*)	8
		862.8 (*a*)	2.7		
		856.3 (*g*), 856.2 (*o*)	80, 147	859.1 (*o* + *g*)	10
		855.1 (*a*)	219	857.5 (*a*)	22
		825–835 (*a*, *o*, *g*)	270 [e]	835.2	76
		823.4 (*a*)	101	824.9 (*a*)	28
		806.5 (*a*)	8.0	806.8 (*a*)	5
		805.5 (*o*), 804.3 (*g*)	88, 112	804.7 (*o* + *g*)	16
		781.0 (*g*), 780.5 (*o*)	312, 357	777.4 (*o* + *g*)	67
		776.1 (*a*)	376	773.8 (*a*)	100
		750–700 [f]		724.9 (*a*)	24
				723.2 (*o* + *g*)	26
				686.1	13
SiC stretch	10	561–640 [g]	60 [e]	638	8
				617.6	11
				612.0	8
sym. SiSi str.	1	442.7 (*g*), 439.1 (*o*)	1.2, 0.9	465 (*o* + *g*)	0.05
(A) [h]		439.1 (*a*)	0.03		
asym. SiSi str.	1	388.0 (*g*), 382.9 (*o*)	2.6, 1.8	415.6 (*o* + *g*)	0.1
(B) [h]		375.6 (*a*)	1.1	406.6 (*a*)	0.2
sym. SiSi str.	1	334.3 (*a*)	0.03		
(A) [h]		327.0 (*o*), 322.5 (*g*)	1.2, 2.9	354.4 (*o* + *g*)	0.1
SiSiC def.	18	25–235 [i]	27 [e]	248.7	2
CSiC def.		[g]		244.3	1
SiSiSi def.	2			222.8	3
				210.0	2
Si–CH_3 torsion	10				
$SiMe_3$ torsion	2				
dihed. torsion	1				

[a] HF/3-21G* frequencies scaled with 0.86. [b] In solid Xe at 12 K; bands assigned to the *anti*, *ortho*, and *gauche* conformers are indicated with *a*, *o*, and *g*, respectively. [c] Number of normal modes for each conformer. [d] Intensities relative to the 774 cm^{-1} band. [e] Calculated intensity of strongest transition in the region. [f] See Figure 8. [g] See Figure 3. [h] Irreducible representations in the C_2 point group. [i] Modes of frequencies below 235 cm^{-1} are mixtures of SiSiC, CSiC, and SiSiSi deformations and methyl, trimethylsilyl, and dihedral torsions. The deformations dominate the higher frequency part of the region and the torsions the lower frequency part. No transition below 175 cm^{-1} has a calculated intensity in excess of 1 km mol^{-1}.

3. Matrix Annealing Experiments: Figure 4 shows the IR spectra from an experiment where Si_4Me_{10} is deposited together with Xe at 10 K and thereafter annealed in steps. The spectrum changes gradually and irreversibly as the temperature is raised, with some peaks increasing and others decreasing in intensity. This indicates that the deposited Si_4Me_{10} is indeed trapped as a mixture of related conformers and we will, for the time being, use the label *A* for the more stable conformer associated with the

© VCH Verlagsgesellschaft mbH, D-69451 Weinheim, 1996
0947-6539/96/0205-0532 $ 15.00+.25/0 Chem. Eur. J. 1996, 2, No. 5

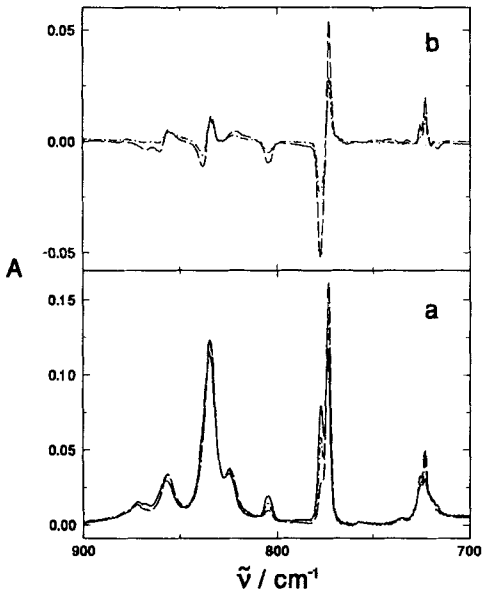

Fig. 4. a) IR absorption spectrum of n-Si_4Me_{10} in solid Xe deposited at 10 K (—) and annealed to steady-state condition at 50 K (- · -) and 65 K (- - -). b) Difference of spectra measured after annealing to 50 K (- · -) or 65 K (- - -) and that recorded immediately after deposition.

growing peaks, and the label *G* for the less stable one, whose peaks decrease. Heating the matrix lowers its viscosity and permits a transformation of *G* into *A*. Even at 65 K, the highest temperature at which the matrix is stable, some *G* conformer remains. Such dispersive kinetics with a whole range of site-dependent activation energies are usual in matrices.

We have not been able to record difference UV spectra as accurately. Even gentle annealing changes the base-line, since light scattering in this spectral region is substantial.

4. Search for a Third Conformer: In the far-IR region calculations predict three groups of weak symmetric and asymmetric Si–Si stretching modes, well separated in frequency from others, and presumably easy to identify. The calculated peak positions for the three calculated conformers are separated by about 5 cm^{-1} (Table 2), and all three have at least some predicted intensity for the asymmetrical stretching mode.

In the Xe matrix, we observe very weak bands at 354, 406, 416, and 465 cm^{-1} (Fig. 5). Their intensities are about three orders of magnitude below those of the most intense mid-IR peaks, and their observation required the use of thick matrices with a low matrix isolation ratio. Only the band at 406 cm^{-1} in the Si–Si stretch region definitely remains after annealing to 70 K. It therefore surely belongs to the *A* conformer. The peaks at 354 and 416 cm^{-1} definitely decrease, and the 465 cm^{-1} band perhaps does as well; this suggests an assignment to the *G* conformer at least for the former two, and possibly for all three. The calculations suggest that the 406 cm^{-1} band is associated with asymmetric Si–Si stretching in the *anti* conformer, and that the other three bands are due jointly to the *ortho* and the *gauche* conformers (asymmetric Si–Si stretching at 416 cm^{-1} and two bands due to symmetric Si–Si stretching at 354 and 465 cm^{-1}).

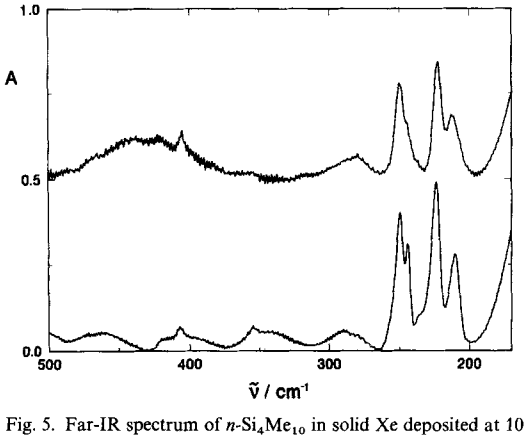

Fig. 5. Far-IR spectrum of n-Si_4Me_{10} in solid Xe deposited at 10 K (bottom) and annealed to 70 K (top, offset by 0.5 absorbance units for clarity).

Repeated attempts to use similar annealing experiments to uncover changes in spectral shape suggestive of the presence of three as opposed to two spectrally distinct conformers failed. Unfortunately, the base-line was frequently heavily distorted by intense interference fringes, which are a fairly common problem in far-IR matrix spectroscopy.

5. Photochemical Transformations: Further evidence for the assignment of the *A* and *G* conformers of Si_4Me_{10} was obtained in irradiation experiments with light preferentially absorbed by one or another conformer. At each wavelength of irradiation the most strongly absorbing conformer is destroyed selectively, leaving a matrix enriched in the less absorbing conformers and in photoproducts. These experiments were only possible with relatively dilute and thin matrices, well penetrated by the UV light, and not on those suitable for measurements in the far IR region.

The dominant photochemical reaction involves a chain abridgement[1] in which octamethyltrisilane (Si_3Me_8) and dimethylsilylene ($SiMe_2$) are formed. Both of these products were easily identified by their characteristic most intense UV and IR bands, which occur at 209 nm and 785 cm^{-1} for Si_3Me_8, based on a comparison with an authentic sample,[24, 25] and 445 nm and 1210 cm^{-1} for $SiMe_2$.[38, 25] An unidentified photoproduct absorbing at 280 nm was also formed, but only in minor amounts, and we were not able to detect any of its IR bands. Peaks with similar absorption were also noted in the irradiation of matrix-isolated Si_3Me_8 and Si_5Me_{12}. They are perhaps due to radicals, known to be produced by irradiation of permethylated oligosilanes in room-temperature solutions.[1]

Figures 6 and 7 present the results of a photodestruction experiment. Figure 6 shows an excerpt from a family of UV spectra taken after increasing times of irradiation. In Figure 7 the corresponding IR spectra of the same sample are shown. In Figures 6a and 7a an Ar matrix containing Si_4Me_{10} is irradiated with an iodine lamp, which primarily emits 48500 cm^{-1} (206.2 nm) radiation. In Figures 6b and 7b, results of similar experiments performed with a cadmium lamp emitting primarily 43710 cm^{-1} (228.8 nm) radiation

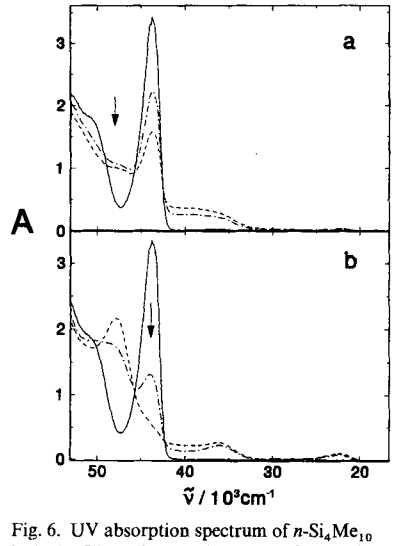

Fig. 6. UV absorption spectrum of n-Si_4Me_{10} in Ar (12 K), as deposited (—) and after irradiation at a) 48500 cm^{-1} or b) 43710 cm^{-1} (- · - 10 min, - - - 20 min). Irradiation wavenumbers are indicated by arrows.

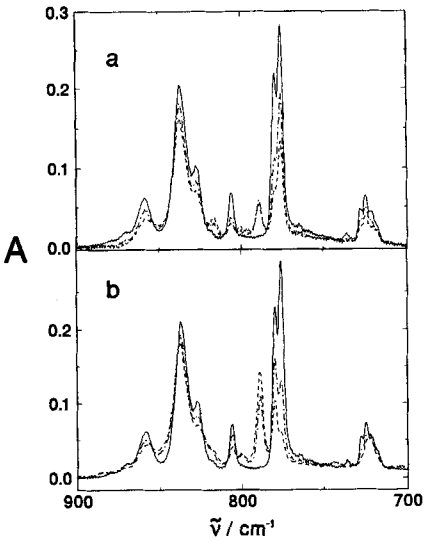

Fig. 7. IR absorption spectrum of *n*-Si_4Me_{10} in Ar (12 K, the same sample as in Fig. 6), as deposited (—) and after irradiation at a) 48500 cm^{-1} or b) 43710 cm^{-1} (- · - 10 min, - - - 20 min).

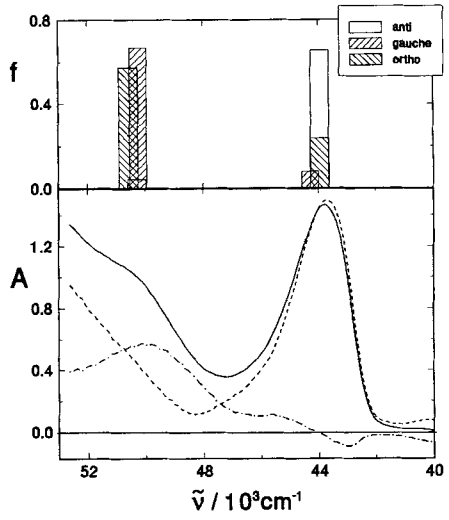

Fig. 9. Observed (—) UV spectrum of the sample of Figure 8 resolved into *anti* (- - -) and *ortho* + *gauche* (- · -) Si_4Me_{10} contributions. Top: calculated (CIS/3-21 G*) wave numbers (scaled by 0.78) and oscillator strengths (*f*) of transitions to the two lowest singlet excited B states of *anti*, *ortho*, and *gauche* Si_4Me_{10}.

are shown. It is clearly seen in the IR spectrum that peaks associated with the *A* conformer (cf. Fig. 3) decrease faster than those associated with the *G* conformer or conformers when irradiated at 43710 cm^{-1}, whereas the opposite is true for high-frequency irradiation at 48500 cm^{-1}. Hence, absorption by the *A* form dominates at low frequency and absorption by the *G* form at high frequency. However, the peaks that belong to the *G* conformer also decrease when irradiated with the Cd lamp, which shows that the low-frequency light (43710 cm^{-1}) is absorbed by the less stable conformer also, albeit weakly.

Figures 6 and 7 also reveal differences in product formation upon irradiation with the two different lamps. The characteristic UV and IR peaks of Si_3Me_8 and $SiMe_2$ grow in parallel to the removal of Si_4Me_{10} when the Cd lamp is used, whereas they are formed only in the early stage of irradiation with the iodine lamp. The light produced by the latter has high enough frequency to photolyze Si_3Me_8. It also destroys $SiMe_2$, and peaks associated with its known matrix photoproduct, 1-methylsilene,[39] are formed (Figs. 6a and 7a).

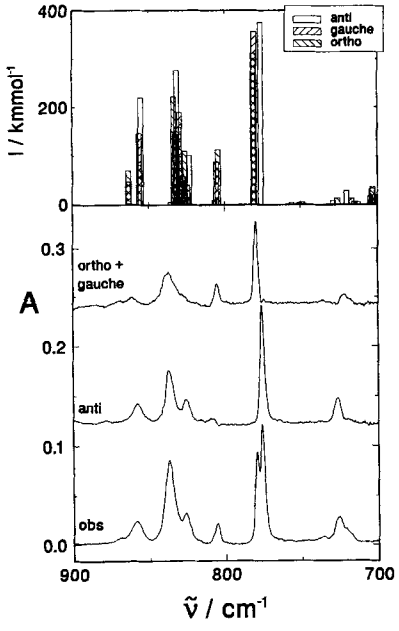

Fig. 8. Observed IR spectrum of Si_4Me_{10} (bottom, in Ar at 12 K) resolved into *anti* and *ortho* + *gauche* contributions (offset for clarity). The top panel shows the calculated IR spectra of *anti*, *ortho*, and *gauche* Si_4Me_{10} (HF/3-21 G*, frequency scaling factor 0.86).

The presence of clearly distinguishable IR peaks of two spectrally distinct conformers, and of the photoproducts, was used to separate their IR and UV spectra (Figs. 8 and 9). The decomposition was achieved by forming linear combinations of the spectrum of the deposited matrix and of the spectra obtained after irradiation with the different lamps at various stages of phototransformation. First, the peaks due to products were removed by forming a suitable linear combination of spectra obtained after irradiation by the two different lamps. The weighting factors were found by inspection of the disappearance of product IR peaks. The resulting spectrum of a mixture of Si_4Me_{10} conformers is linearly independent of the spectrum of the originally deposited matrix. Next, linear combinations of these two spectra are formed until peaks due to the *A* or the *G* conformer just disappear, leaving the spectrum of the pure *G* or *A* conformer, respectively.

The UV spectra of the *A* and *G* forms (Fig. 9) were derived from the spectra recorded on the same samples by forming linear combinations with the weighting factors deduced from the above analysis of the IR spectra. While it could be argued that the IR matrix spectra of *A* and *G* are so similar that the two species represent two distinct matrix sites and not two conformers, the very different UV spectra cannot be accounted for in this manner and prove that *A* and *G* differ in more than just the matrix environment.

The spectral decomposition relies on the assumption that the system is composed of three and only three spectrally distinct principal components, namely, *A*, *G* + *O*, and photoproducts. It works perfectly in the IR region shown (Fig. 8) and gives a reasonable result for the UV spectrum (Fig. 9), although in the latter some base-line distortion is due to photoproducts that are not formed in a simple 1:1 relation to Si_3Me_8 and $SiMe_2$. Since the photodestruction experiment showed that *G* + *O* absorbs at 43710 cm^{-1}, the weak shoulder reproducibly present near 45500 cm^{-1} in the spectrum attributed to *G* + *O* is surely real, even though its shape may be somewhat distorted in Figure 9.

6. IR Spectra, Comparison with Calculations: The calculated IR spectra (HF/3-21 G*) for *anti*, *ortho*, and *gauche* Si_4Me_{10} are shown in Figure 3. The critical spectral region is also shown in Figure 8, together with the decomposed spectra derived from experiment. The agreement between the spectrum calculated for *a* and that observed for *A*, and the agreement between the virtually identical mid-IR spectra calculated for *o* and *g* and that observed for *G*, are convincing enough to be used as a basis for spectral assignments. In the 900–300 cm^{-1} region quite a few observed bands can be assigned separately to either the *anti* or

© VCH Verlagsgesellschaft mbH, D-69451 Weinheim, 1996
0947-6539/96/0205-0534 $ 15.00+.25/0 Chem. Eur. J. 1996, 2, No. 5

gauche/ortho conformers. Table 2 provides a general summary of the observed and calculated frequencies and their assignments.

7. UV Spectra, Comparison with Calculations: The UV spectra of the *anti* and *ortho/gauche* conformers of Si_4Me_{10} obtained from the spectral resolution are shown in Figure 9. They are qualitatively similar to but quantitatively more reliable than the spectra reported in our preliminary communications.[24, 25] The absorption of the *anti* form, with its intense peak at 43700 cm^{-1}, represents no surprise. This is the peak that dominates the known ordinary solution spectrum. In contrast, the absorption of the *ortho/gauche* conformer contains not only the anticipated fairly intense peak at 49700 cm^{-1}, responsible for the shoulder familiar from ordinary solution spectra, but also a second weaker peak at 44–46000 cm^{-1}, usually hidden by the intense absorption of the *anti* form.

Figure 9 also shows results of CIS/3-21G* calculations of excitation energies, scaled by a factor of 0.78. Excited state calculations with such small CI and poor basis set have only qualitative significance, but it is encouraging that the trends are essentially identical with those for Si_4H_{10}.[9, 27] Within the acknowledged limitations, the agreement with the observed difference between the two conformers is satisfactory and suggests that the rendition of the conformational dependence of the excited-state wave functions provided by this level of calculation is meaningful. Figure 10 shows the computed excitation energy

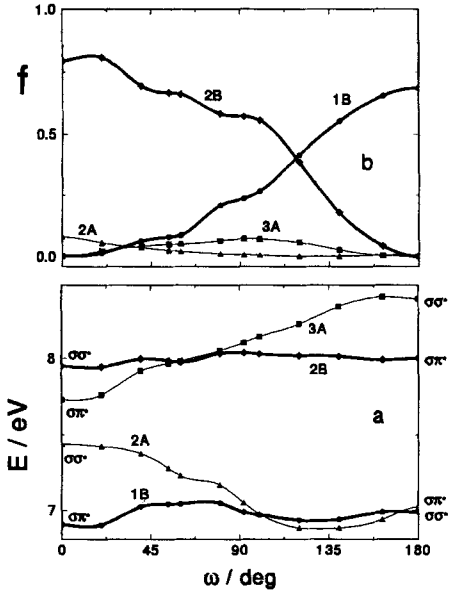

Fig. 10. Calculated (CIS/3-21G*) singlet a) excitation energies and b) oscillator strengths of Si_4Me_{10} as a function of the SiSiSiSi dihedral angle ω.

and oscillator strength for Si_4Me_{10} as a function of the backbone dihedral angle. Since the size of the molecule precludes the inclusion of diffuse functions in the basis set, Rydberg states are missing in the results. In condensed media these are ordinarily not observable, and we expect the results to be qualitatively significant for predominantly valence states.

The calculation places transitions to two A states and two B states into the region of interest. Because of the lower transition probability to the A states in one-photon absorption, the B states are the ones most likely to be observed. The excitation energies of the two lowest transitions are calculated to be almost independent of the dihedral angle, whereas the oscillator strengths vary significantly. At the *anti* geometry the transition to the 1 B state is intense and the transition to the 2 B state is very weak. For a twisted geometry both transitions into B states are predicted to have fairly high intensities, with the second being stronger at dihedral angles smaller than 120°. This agrees with the observation that the UV spectra of the *anti* and twisted conformers overlap at all wavelengths, and that the *anti* conformer dominates the absorption at lower and the twisted ones at higher energies.

The computed behavior is due to an avoided crossing between the two lowest B states as the dihedral angle is varied from 180 to 0°. At these two angles, the molecule has a plane of symmetry and its orbitals can be classified as being of σ or π symmetry. Inspection of the wave functions shows that the lower B state at $\omega = 180°$ and the upper B state at $\omega = 0°$ are of the $\sigma\sigma^*$ type and intense, while the other B state in each case is of the $\sigma\pi^*$ type and very weak. A true crossing of the two B states with changing dihedral angle is avoided, since at intermediate dihedral angles, the plane of symmetry is absent. Thus, in the *anti* conformer, one expects to observe a single intense transition at low energies, and a weak upper transition. In either the *ortho* or the *gauche* conformer, one expects to observe a weaker transition at low energies and an intense one at higher energies. In a hypothetical *syn* conformer ($\omega = 0°$), we would expect an extremely weak transition at low energies and a very intense one at higher energies.

The A states also are one of the $\sigma\sigma^*$ type and one of the $\sigma\pi^*$ type, and are calculated to undergo a similar avoided crossing. We have no experimental evidence for their presence, and in view of their very low calculated absorption cross-sections, this is not surprising. Perhaps they could be detected by two-photon absorption spectroscopy.

Discussion

Ground-State Conformations: The first calculations that suggested that something is out of the ordinary in the conformational behavior of permethylated linear oligosilanes and predicted the existence of six conformational minima as a function of the SiSiSiSi dihedral angle used the empirical MM2[40] and semiempirical MNDO/2[41] methods. These levels of calculation are not very reliable. For instance, the latter also predicted six minima for Si_4H_{10}, where there is little doubt that there are only three in reality.[36]

The unusual results for permethylated chains were therefore apparently not taken very seriously. Yet, the present work does not leave much doubt that they were correct in the case of Si_4Me_{10}, whose backbone indeed has at least six conformational minima. This conviction is based not only on our calculations for these molecules, which show no indication whatever that an improvement of the wave function quality will restore the usual situation with only three or four minima, but also on the computational[10] and experimental[11] evidence that was obtained for the existence of three distinct conformers of C_4F_{10}.

The geometries of two of the minima are those anticipated for the usual pair of *gauche* enantiomers, with a dihedral angle of about $\pm 60°$, and another two are those anticipated for the usual pair of *anti* enantiomers, with a dihedral angle of about $\pm 165°$. In *n*-butane and *n*-tetrasilane, there is only one *anti* minimum, with a dihedral angle of 180°, but in substituted hydrocarbon chains the *anti* minimum often splits into a pair of enantiomeric minima separated by a very small barrier, presumably due to 1,3-interactions.

The unusual conformation is the one with dihedral angles of about $\pm 90°$, for which we have proposed[11] the designation "*ortho*". Previous ab initio calculations identified this value of dihedral angle as a minimum,[24, 26, 27] but the authors assumed that this was merely a distorted *gauche* conformer, rather than a separate minimum.

Although there is at present no experimental evidence for the existence of three conformational forms of Si_4Me_{10} itself, the available crystal structures of permethylated silicon chains are certainly compatible with ± 60, ± 90, and $\pm 165°$ being the favored values of the SiSiSiSi dihedral angle. Both the monocyclic ring $Si_{16}Me_{32}$[42] and the branched structures $[(Me_3Si)_3SiSiMe_2]_3SiMe$,[43] $[(Me_3Si)_3SiSiMe_2]_2$,[44] $[(Me_3Si)_2SiMeSiMe_2]_3SiH$,[45] and $[(Me_3Si)_2SiMe]_3SiMe$[45] exhibit dihedral angles that cluster around the values 40–60, 80–100, and 150–180°. In the solid polymer $(SiMe_2)_n$, the dihedral angle is 180°,[46] but since the calculated energy increase from the dihedral angle of 165 to 180° is only about 0.4 kcal mol^{-1}, this discrepancy could easily be due to crystal packing forces.

The energies calculated for the three conformers of Si_4Me_{10} are very close. The MP2/6-311 G** calculation predicts the *anti* minimum to be the most stable. The *gauche* minimum lies 0.17 kcal mol^{-1} and the *ortho* minimum 0.50 kcal mol^{-1} higher, and this can be compared with the results of lower quality ab initio calculations (Table 1), and with the earlier MNDO/2 results, which place the *gauche* and *ortho* energies 1.4 and 1.1 kcal mol^{-1} above the *anti* minimum, respectively.[41] These relative energies apply to isolated molecules and do not reflect differential stabilization in the solid. We would expect the *anti* form, which is the most spatially extended, to be generally stabilized the most by van der Waals interactions with solute molecules in condensed phase, but more specific interactions related to the size of host matrix cavities, etc., may complicate matters.

The calculated barriers are very small as well. It takes a little over 0.5 kcal mol^{-1} to go from the *ortho* minimum to the nearby *gauche* minimum, and a little less than 1 kcal mol^{-1} to go to the nearby *anti* minimum. The interconversion of the two *anti* forms involves a barrier of only about 0.4 kcal mol^{-1}, and the direct interconversion of the two *gauche* forms, a barrier of a little less than 3 kcal mol^{-1}. Assuming reasonable frequency factors, these barriers are too small to account for the stability of the observed IR spectra to annealing, and we believe that the rate of interconversion of the conformers in the matrix is dictated by the viscosity of the medium. This is supported by the very nonexponential kinetic behavior observed. The only minute adjustment needed for the transformation from an *ortho* to a *gauche* geometry makes it likely that much of the *ortho* form present in the gas phase is lost by conversion into the *gauche* form in the process of matrix trapping.

In spite of the fairly unambiguous computational results, the data for C_4F_{10}, and the supporting evidence from the X-ray structures of other permethylated structures containing silicon chains, it clearly remains most desirable to provide a direct experimental proof of the existence of three distinct conformers in Si_4Me_{10} itself. In our hands, the tool employed in the present study, IR spectroscopy, turned out not to be up to the task. Fortunately, we could decompose the IR and UV spectra at least into those of the *anti* form and those of the sum of the *gauche* and *ortho* forms, by annealing and by selective photodestruction. Each has pros and cons. The former does not increase the total number of constituents in the matrix but tends to change the base-line, making spectral subtractions less reliable. The latter does not perturb the base-line, but introduces new constituents.

Infrared Spectra: The mid-IR region is calculated to contain no peaks that are at distinctly different frequencies in the *gauche* and the *ortho* form, with the largest separations on the order of 1 cm^{-1}. This is not surprising, considering their extremely close structural similarity, the involvement of substituent motions in the normal modes that occur in this spectral region, and the ability of the relatively heavy silicon atoms to act as vibrational insulators. The frequencies calculated for the spectrum of the *anti* form are nearly identical as well, with the exception of the intense vibration near 780 cm^{-1}. Even this largest calculated difference amounts only to 4.5 cm^{-1} (observed, 3.6 cm^{-1}).

The far-IR peaks due to vibrations of the silicon skeleton itself are more sensitive to molecular conformation, but are orders of magnitude weaker. To observe them at all, we used thick and concentrated matrices, impenetrable to UV light and precluding the use of the selective photodestruction method. The annealing method failed to identify a third conformer, both because uniform annealing of thick matrices is difficult and because much annealing and loss of the least stable *ortho* conformer probably occur during the initial deposition, when it is hard to keep the surface of a thick matrix at the desired low temperature. After all, in our experiments with the three conformers of C_4F_{10}, the *ortho* form disappeared already upon annealing from 12 to 18 K.[11] We concluded that it would be preferable to look for the third conformer of Si_4Me_{10} by Raman spectroscopy, where the intensities of low-frequency skeletal vibrations are calculated to be very high.

Si_4Me_{10} has 126 normal modes. The silicon backbone alone has six normal modes, namely, three stretches, two deformations, and one torsion. The other 120 normal modes involve methyl groups. Of these, 60 are pure methyl fundamentals—30 stretches in the range 2850–3000 cm^{-1} and 30 deformations in the range 1200–1450 cm^{-1} (Table 2 and Fig. 3). Little information about the conformers could be extracted from these methyl vibrations.

The strongest IR transitions are found in the SiCH deformation/SiC stretching region between 900 and 600 cm^{-1}. These are generally mixtures of SiCH deformations and SiC stretches, with the former dominating at higher frequencies and the latter at lower frequencies. Some of the bands are separated enough to make assignments to the *anti* conformer and jointly to *ortho* and *gauche*; this implies that motions of the silicon backbone are involved to some degree. The best separation is found for the mode close to 780 cm^{-1}, and these are the bands that have been used to guide the spectral decomposition. There are other bands in this region with similar separation between the individual conformers, but most are overlapped by other transitions and could not be observed individually. Those found to be separated enough are listed in Table 2. Other than the involvement of the silicon backbone in the normal modes, we have not found any particular feature that causes some transitions to be more separated in the individual conformers than others.

The agreement between calculations and experimental observations is surprisingly good, considering the size of the molecule. After scaling the calculated frequencies with a single factor of 0.86 (determined from the strongest band at 776 cm^{-1}), most calculated frequencies fall within 20 cm^{-1} of the observed bands. The largest deviations are found for the modes that are mostly of stretching character (CH, SiC, and SiSi stretches), which are all predicted to be too low, in agreement with experience from other systems where stretching frequencies often require a larger scaling factor than deformations in order to agree with observation. This suggests that the region between 900 and 700 cm^{-1} is dominated by SiCH deformations and the region between 700 and 600 cm^{-1} by SiC stretches, since the

© VCH Verlagsgesellschaft mbH, D-69451 Weinheim, 1996
0947-6539/96/0205-0536 $ 15.00+.25/0 Chem. Eur. J. 1996, 2, No. 5

agreement is good in the former region and increasingly worse in the latter.

A final comment pertains to the observed separated spectra of the *anti* conformer (Fig. 8). The normal mode calculated for the weak band observed at 806.5 cm^{-1} is of gerade symmetry for the hypothetical centrosymmetric *anti* conformer, and would be expected to have zero intensity if the *anti* conformer were planar. The fact that this band has observable intensity agrees with its computed nonplanarity ($\omega \neq 180°$). The proof is not absolute, since the intensity could also be induced by a matrix perturbation.

Ultraviolet Spectra: It is commonly believed that the all-*anti* form of a linear peralkylated silicon chain has the lowest singlet excitation energy of all conformers,[1] and that the observed excited state is of $\sigma\sigma^*$ nature, except perhaps in the shortest chains where it could be $\sigma\pi^*$ or Rydberg.[47] Our initial results[24] on the spectral separation of the *anti* and the *gauche* conformers of Si_4Me_{10} supported this view. The intense peak of the *anti* form was seen at 43900 cm^{-1}, and that of the *gauche* form at 48500 cm^{-1}. Although we now believe that the *gauche* peak is due to overlapping contributions from two conformers, *gauche* and *ortho*, it is quite broad and a small difference in their excitation energies could be easily accommodated. Subsequent results for Si_5Me_{12} suggested the presence of three conformers in this five-silicon chain, at the time believed to be *aa*, *ag*, and g^+g^+, and supported the notion that the first intense excitation in the twisted conformers occurs at higher energies. A comparison of results for chains from two to five silicon atoms suggested that the addition of an *anti* link extends the conjugated system and the addition of a *gauche* link does not, at least as judged by the position of the first intense UV peak.[25]

A simple elaboration of the Sandorfy C model,[20] dubbed the ladder C model[24] since the topology of interactions included resembled a ladder, accounted for the observed energies of excitation.[26] With optimized values of the resonance integrals, the agreement was quantitative for all conformers of the Si_2Me_6–Si_5Me_{12} series, as well as the *anti* conformers of all known longer chains up to $Si_{16}Me_{34}$. At this point, it appeared that it would be possible to use this still quite simple four-parameter model to account for the positions of the first intense peaks of all conformers of linear Si_nMe_{2n+2} chains of all lengths.

This high degree of putative understanding was short lived. Two vexing problems refused to disappear upon further elaboration. First, the optimized value of the 1,4 resonance integral for the *gauche* geometry required in the ladder C model was more negative than expected from simple considerations of its relation to the integral for the *anti* geometry based on the angular dependence of orbital overlap[26] or from consideration of the elements of the Hartree–Fock operator in the basis of natural hybrid orbitals.[9] Its value corresponded to expectations for the *syn* geometry, with a zero SiSiSiSi dihedral angle. Second, preliminary results for the twisted conformers of Si_6Me_{14} did not fit the predictions of the model well.[26, 27] While it could be argued that parameters in semiempirical models frequently hide a large number of neglected factors and do not always have a simple physical interpretation and the expected value, and while the number of conformers expected for Si_6Me_{14} is large enough to make the preliminary spectral separations suspect, the doubts prompted additional investigation. They were strengthened after our CASSCF/CIS/ccVDZ calculations for Si_4H_{10} failed to show any significant increase in the energy of the lowest excited singlet state upon going from the *anti* to twisted geometries.[26] When it became clear that various improvements of the ab initio method still did not show the expected qualitative behavior at all, we used a simpler ab initio method (CIS/6-31 G**) to calculate the energies and intensities of several electronic transitions of Si_4H_{10} at a large number of geometries along the bond-twisting path.[9, 27]

The resulting correlation diagram for Si_4H_{10} was nearly identical with that computed presently for the permethylated analogue, Si_4Me_{10} (Fig. 10). We are aware of the shortcomings of the CIS level of calculation and are currently repeating the calculations for Si_4H_{10} at higher levels of theory, but for the moment assume that the new results will not change the diagram significantly, and that the results shown in Figure 10 are valid.

Both in Si_4H_{10} and in Si_4Me_{10}, for SiSiSiSi dihedral angles close to 180° (the *anti* geometry), the ab initio calculation supports the basic assumption of all the simple models and assigns the lowest excited singlet state as $\sigma\sigma^*$ (B_u symmetry, long-axis polarized) and the transition into it as strongly allowed, corresponding to the transition actually observed. The wave function of the excited state correspond well to expectations based on the simple ladder C or Sandorfy C models. However, for dihedral angles close to 0° (*syn* geometries), the ab initio calculation assigns the lowest strongly allowed $\sigma\sigma^*$ transition to the second excited state (B_2, long axis polarized), at significantly higher energies. The wave functions of this state again correspond to expectations based on the simple models, and those of the lower excited singlets do not. The unobserved transitions into these lower states are calculated to be of low intensity and could easily have been missed in the observed spectra. If the only observed conformations of the silicon chains were *anti* and *syn*, the ladder C model could then still be used successfully; it would predict the excitation energy of the first intense singlet–singlet transition and say nothing about the weak transitions at higher energies in the *anti* form and at lower energies in the *syn* form.

In reality, however, the conformations populated next to *anti* are at intermediate dihedral angles, *gauche* and *ortho*. At these geometries, symmetry is lower, and as noted in the Results section, an avoided crossing of the $\sigma\pi^*$ and $\sigma\sigma^*$ B symmetry states of the planar forms takes place upon proceeding from the *syn* to the *anti* geometry. The ab initio wavefunctions computed for both the lowest and the next higher excited singlet of B symmetry at these intermediate geometries therefore contain some of the strongly allowed backbone excitation treated by the simple models ("$\sigma\sigma^*$"), and some of the weakly allowed excitations involving bonds to lateral substituents and absent in the simple models ("$\sigma\pi^*$"). Because of the strongly avoided crossing, the energies of both the lower and the upper resulting B state are nearly independent of the twist angle. It is thus the intensity and not the energy of the lowest two B states of the tetrasilane chain that is conformation-sensitive.

This proposal accounts for the angular independence of the computed lowest excitation energy observed in our earlier ab initio work. It also accounts for the unexpected value of the 1,4 resonance integral for the *gauche* link: we took the excitation energy of the intense, that is, the second excited B state of the *gauche* form for the fitting. This energy is that which would be observed for the *syn* form, and it is in the *syn* form that the wave function of the observed state is of the backbone $\sigma\sigma^*$ type assumed in the ladder C model. Although the vexing problems with the ladder C model are thus explained, it is clear that a description of the electronic structure of saturated chains should not be restricted to the backbone. We are continuing our efforts to develop a parameter set for the next more complicated Hückel model, ladder H, which considers the electrons of the bonds to substituents in addition to those in the backbone. Even the simplest picture of σ conjugation will be quite complex if one insists on reproducing the effects of conformation.

In conclusion, we emphasize the fact that the new spectroscopic results presented in Figure 9 provide the first piece of experimental evidence for the revised interpretation of the conformational dependence of the UV spectrum of decamethyl-*n*-tetrasilane based on CIS calculations[9, 27] (Fig. 10), according to which changes in the SiSiSiSi dihedral angle affect band intensities rather than energies. This is likely to be valid for other substituted *n*-tetrasilanes as well. For longer silicon chains, the state reversal between the *syn* and *anti* planar geometries might not take place, since excitation energies of $\sigma\sigma^*$ type drop faster with increasing chain length than $\sigma\pi^*$. In systems for which the "$\sigma\sigma^*$" state is the lowest at all conformations of interest, the ladder C model might be adequate.

Conclusions

The present study offers 1) computational evidence (MP2/6-31G*) that permethyltetrasilane has three rather than the usual two pairs of enantiomeric conformers at very similar energies (*gauche*, *ortho*, and *anti*); 2) separated IR spectra of the *gauche* and the *anti* conformers and their assignment in terms of modes of vibration (based on HF/3-21G* calculations); 3) experimental evidence that, in a matrix, the *anti* conformer is the lowest in energy; 4) separated UV spectra of the *gauche* (+ *ortho*) and the *anti* conformers, the former of which does not fit traditional expectations and supports the recent reassignment based on $\sigma\pi^* - \sigma\sigma^*$ mixing; 5) the conclusion that the usual Sandorfy C as well as the more recent ladder C models are incapable of accounting for the dependence of σ conjugation in saturated chains on their length and conformation, the more complex ladder H model being the simplest that might be able to do so.

Note added in proof: A recent report on the crystal structures of several branched oligosilanes classified conformations in three families: *gauche* ($\omega = 30-64°$), *ortho* ($\omega = 80-106°$), and *anti* ($\omega = 131-177°$); J. B. Lambert, J. L. Pflug, J. M. Denari, *Organometallics* **1996**, *15*, 615.

Acknowledgement: This work was supported by USARO grant DAAH04-94-G-0018, funded jointly with NSF/DMR, NSF computer grant CHE-9412767, and a Pittsburgh Supercomputing Center Grant CHE-940016P. Technical assistance by K. R. Vanderveen is greatly appreciated. B. A. is grateful to the Natural Science Research Council of Sweden for a fellowship.

Received: August 8, 1995 [F185]
Revised version: November 29, 1995

[1] R. D. Miller, J. Michl, *Chem. Rev.* **1989**, *89*, 1359.
[2] For examples of recent experimental studies, see: R. D. Miller, G. M. Wallraff, M. Baier, P. M. Cotts, P. Shukla, T. P. Russell, F. C. De Schryver, D. Declercq, *J. Inorg. Organomet. Polym.* **1991**, *1*, 505. F. C. Schilling, A. J. Lovinger, D. D. Davis, F. A. Bovey, J. M. Zeigler, *J. Inorg. Organomet. Polym.* **1992**, *2*, 47; *Macromolecules* **1993**, *26*, 2716. T. Itoh, I. Mita, *ibid.* **1992**, *25*, 479. E. K. KariKari, A. J. Greso, B. L. Farmer, R. D. Miller, J. F. Rabolt, *ibid.* **1993**, *26*, 3937. C.-H. Yuan, R. West, *ibid.* **1994**, *27*, 629. K. Sakamoto, M. Yoshida, H. Sakurai, *ibid.* **1994**, *27*, 881.
[3] For examples of computational studies, see: J. R. Damewood, Jr., R. West, *Macromolecules* **1985**, *18*, 159. B. L. Farmer, J. F. Rabolt, R. D. Miller, *Macromolecules* **1987**, *20*, 1167. J. V. Ortiz, J. W. Mintmire, *J. Am. Chem. Soc.* **1988**, *110*, 4522. J. W. Mintmire, *Phys. Rev. B* **1989**, *39*, 13350. H. Teramae, K. Takeda, *J. Am. Chem. Soc.* **1989**, *111*, 1281. C. X. Cui, A. Karpfen, M. Kertesz, *Macromolecules* **1990**, *23*, 3302. M. Jalali-Heravi, S. P. McManus, S. E. Zutaut, J. K. McDonald, *Chem. Mater.* **1991**, *3*, 1024. W. J. Welsh, *Adv. Polym. Technol.* **1993**, *12*, 379.
[4] E.g., H. Tachibana, Y. Kawabata, Y. Moritomo, S.-Y. Koshihara, Y. Tokura, R. D. Miller, *Mol. Cryst. Liq. Cryst.* **1992**, *217*, 65.
[5] K. A. Klingensmith, J. W. Downing, R. D. Miller, J. Michl, *J. Am. Chem. Soc.* **1986**, *108*, 7438.
[6] N. Matsumoto, H. Teramae, *J. Am. Chem. Soc.* **1991**, *113*, 4481, and references therein.
[7] J. V. Ortiz, C. M. Rohlfing, *Macromolecules* **1993**, *26*, 7282.
[8] C. A. Ernst, L. A. Allred, M. A. Ratner, *J. Organomet. Chem.* **1979**, *178*, 119.
[9] H. Teramae, J. Michl, *Mol. Cryst. Liq. Cryst.* **1994**, *256*, 149.
[10] G. D. Smith, R. L. Jaffe, D. Y. Yoon, *Macromolecules* **1994**, *27*, 3166.
[11] B. Albinsson, J. Michl, *J. Am. Chem. Soc.* **1995**, *117*, 6378. B. Albinsson, J. Michl, *J. Phys. Chem.* **1996**, *100*, 3418.
[12] H. Teramae, F. Neumann, J. W. Downing, J. Michl, unpublished results.
[13] A. E. Reed, F. Weinhold, *Israel J. Chem.* **1991**, *31*, 277, and references therein.
[14] A. Streitwieser, Jr., *Molecular Orbital Theory for Organic Chemists*, Wiley, New York, NY, 1961.
[15] M. J. S. Dewar, R. C. Dougherty, *The PMO Theory of Organic Chemistry*, Plenum Press, New York, NY, 1975.
[16] L. Salem, *The Molecular Orbital Theory of Conjugated Systems*, Benjamin, New York, NY, 1966.
[17] R. Hoffmann, *Acc. Chem. Res.* **1971**, *4*, 1.
[18] AM1: M. J. S. Dewar, E. G. Zoebisch, E. F. Healy, J. J. P. Stewart, *J. Am. Chem. Soc.* **1985**, *107*, 3902. M. J. S. Dewar, C. Jie, *Organometallics* **1987**, *6*, 1486. MNDO: M. J. S. Dewar, W. Thiel, *J. Am. Chem. Soc.* **1977**, *99*, 4899. M. J. S. Dewar, M. L. McKee, H. S. Rzepa, *ibid.* **1978**, *100*, 3607. SINDO: D. N. Nanda, K. Jug, *Theor. Chim. Acta* **1980**, *57*, 95. K. Jug, R. Iffert, J. Schultz, *Int. J. Quantum Chem.* **1987**, *32*, 265. J. Li, P. Correa de Mello, K. Jug, *J. Comput. Chem.* **1992**, *13*, 85.
[19] A. E. Reed, L. A. Curtiss, F. Weinhold, *Chem. Rev.* **1988**, *88*, 899, and references therein.
[20] C. Sandorfy, *Can. J. Chem.* **1955**, *33*, 1337.
[21] Y.-P. Sun, Y. Hamada, L. M. Huang, J. Maxka, J.-S. Hsiao, R. West, J. Michl, *J. Am. Chem. Soc.* **1992**, *114*, 6301.
[22] Y.-P. Sun, J. Michl, *J. Am. Chem. Soc.*, **1992**, *114*, 8186.
[23] Y.-P. Sun, G. M. Wallraff, R. D. Miller, J. Michl, *J. Photochem. Photobiol.* **1992**, *62*, 333.
[24] H. S. Plitt, J. Michl, *Chem. Phys. Lett.*, **1992**, *198*, 400.
[25] H. Plitt, V. Balaji, J. Michl, *Chem. Phys. Lett.*, **1993**, *213*, 158.
[26] H. S. Plitt, J. W. Downing, M. K. Raymond, V. Balaji, J. Michl, *J. Chem. Soc. Faraday Trans.*, **1994**, *90*, 1653.
[27] H. S. Plitt, J. W. Downing, H. Teramae, M. K. Raymond, J. Michl, *ACS Symposium Series* 579 (Eds.: H. Ito, S. Tagawa, K. Horie), *Polymeric Materials for Microelectronic Applications, Science and Technology*; American Chemical Society, Washington, DC, 1994; Chapter 30, p. 376.
[28] Synthesized according to H. Sakurai, M. Yamamori, M. Yamagata, M. Kumada, *Bull. Chem. Soc. Jpn.* **1968**, *41*, 1474, and purified by preparative GC (10% SE-30 on 80/100W Chromosorb; 0.5 m column).
[29] On-Line Instrument Systems, Bogart, Georgia.
[30] The Turbomole program system from Biosym Technologies of San Diego, CA: R. Ahlrichs, M. Bär, M. Häser, H. Horn, C. Kölmel, *Chem. Phys. Lett.* **1989**, *162*, 165. F. Haase, R. Ahlrichs, *J. Comput. Chem.* **1993**, *14*, 907–912. M. Häser, R. Ahlrichs, *ibid.* **1989**, *10*, 104.
[31] Gaussian 92, Revision C, M. J. Frisch, G. W. Trucks, M. Head-Gordon, P. M. W. Gill, M. W. Wong, J. B. Foresman, B. G. Johnson, H. B. Schlegel, M. A. Robb, E. S. Replogle, R. Gomperts, J. L. Andres, K. Raghavachari, J. S. Binkley, C. Gonzalez, R. L. Martin, D. J. Fox, D. J. Defrees, J. Baker, J. J. P. Stewart, J. A. Pople, Gaussian, Pittsburgh PA, 1992.
[32] M. S. Gordon, J. S. Binkley, J. A. Pople, W. J. Pietro, W. J. Hehre, *J. Am. Chem. Soc.* **1982**, *104*, 2797. J. S. Binkley, J. A. Pople, W. J. Hehre, *ibid.* **1980**, *102*, 939. W. J. Pietro, M. M. Francl, W. J. Hehre, D. J. DeFrees, J. A. Pople, J. S. Binkley, *ibid.* **1982**, *104*, 5039.
[33] P. C. Hariharan, J. A. Pople, *Theor. Chim. Acta* **1973**, *28*, 213. R. Ditchfield, W. J. Hehre, J. A. Pople, *J. Chem. Phys.* **1971**, *54*, 724. W. J. Hehre, R. Ditchfield, J. A. Pople, *ibid.* **1972**, *56*, 2257. M. S. Gordon, *Chem. Phys. Lett.* **1980**, *76*, 163.
[34] R. Krishnan, J. S. Binkley, R. Seeger, J. A. Pople, *J. Chem. Phys.* **1980**, *72*, 650. A. D. McLean, G. S. Chandler, *ibid.* **1980**, *72*, 5639.
[35] M. J. S. Dewar, S. Kirschner, *J. Am. Chem. Soc.* **1971**, *93*, 4292.
[36] A. Haaland, K. Rypdal, H. Stüger, H. V. Volden, *Acta Chem. Scand.* **1994**, *48*, 46. B. Albinsson, H. Teramae, H. S. Plitt, L. M. Goss, H. Schmidbauer, J. Michl, *J. Phys. Chem.*, in press.
[37] P. Huber-Wälchli, *Ber. Bunsenges. Phys. Chem.* **1978**, *82*, 10. M. E. Squillacote, R. S. Sheridan, O. L. Chapman, F. A. L. Anet, *J. Am. Chem. Soc.* **1979**, *101*, 3657. See also B. R. Arnold, V. Balaji, J. W. Downing, J. G. Radziszewski, J. J. Fisher, J. Michl, *ibid.* **1991**, *113*, 2910, and references therein.
[38] T. J. Drahnak, J. Michl, R. West, *J. Am. Chem. Soc.* **1979**, *101*, 5427; G. Raabe, H. Vančik, R. West, J. Michl, *J. Am. Chem. Soc.* **1986**, *108*, 671.
[39] T. J. Drahnak, J. Michl, R. West, *J. Am. Chem. Soc.* **1981**, *103*, 1845.
[40] W. J. Welsh, L. Debolt, J. E. Mark, *Macromolecules* **1986**, *19*, 2987.
[41] W. J. Welsh, W. D. Johnson, *Macromolecules*, **1990**, *23*, 1881.
[42] F. Shafiee, K. J. Haller, R. West, *J. Am. Chem. Soc.* **1986**, *108*, 5478.
[43] J. B. Lambert, J. L. Pflug, C. L. Stern, *Angew. Chem. Int. Ed. Engl.* **1995**, *34*, 98.
[44] J. B. Lambert, J. L. Pflug, A. M. Allgeier, D. J. Campbell, T. B. Higgins, E. T. Singewald, C. L. Stern, *Acta Crystallogr. Sect. C: Cryst. Struct. Commun.* **1995**, *C51*, 713.
[45] J. L. Pflug, Ph.D. Dissertation, Northwestern Univ., Evanston, IL, 1994.
[46] A. J. Lovinger, D. D. Davis, F. C. Schilling, F. J. Padden, Jr., F. A. Bovey, J. M. Zeigler, *Macromolecules*, **1991**, *24*, 132.
[47] V. Balaji, J. Michl, *Polyhedron* **1991**, *10*, 1265.

© VCH Verlagsgesellschaft mbH, D-69451 Weinheim, 1996